Sodium Binding and Translocation by the Na^+/K^+ ATPase

Josh Levitz

5/1/2009

Honors Thesis in Biology

Abstract:

The Na/K pump, a P-type ATPase, uses the energy of ATP hydrolysis to export three sodium ions and import two potassium ions into the cell in each cycle. Ions enter from either side of the membrane, bind specific binding sites, become occluded, and are released to the other side. When deprived of potassium ions, the pump is restricted to sodium translocation, a voltage-dependent, sequential process. In this work, I have further elucidated the transitions that occur in sodium translocation. I have provided evidence for a three-step mechanism and have characterized the voltage-dependence of the slow and medium charge components of translocation. Furthermore, using mutations specific to sodium binding sites I, II, and III, I have found clues to how the steps of sodium translocation are mediated at a structural level. Ultimately, I propose that site III produces the slow component of charge with sites I and II producing the medium and fast components respectively.

Introduction:

The Na/K ATPase (Na/K pump) is a P-type ATPase that uses ATP hydrolysis to export three sodium ions (Na+) out of and import two potassium ions (K+) into the cell in each cycle. This ion "pumping" is deemed electrogenic due to the net positive charge (measured as outward current) that is pumped out of the cell. This polarizes the membrane leading to a net negative charge inside the cell relative to the outside. Na/K pump function has been shown to lie at the heart of such diverse physiological functions as excitability of neurons, control of intracellular pH, control of cell size, and cardiac electrical activity (1).

In the Post-Albers transport cycle (fig. 1a), first described in 1972, Na+ and K+ are alternately bound and occluded in E1 and E2 conformations that are driven by ATP hydrolysis. This transport cycle, under physiological conditions, occurs 100 times per second and consumes 20-30% of the ATP produced in the average cell (2). Importantly, due primarily to the attraction of extracellular Na+ to pump binding sites (which opposed forward "pumping") within the membrane at negative potentials, the Na/K pump is inherently voltage-dependent (3). This voltage-dependence lies at the heart of the biophysical characterization of pump activity. It has been previously shown that, when deprived of K+ on the external side of the membrane and supplied internal ATP, the Na/K pump may be limited to steps of Na+ translocation (4). In Na+ translocation, Na+ is exchanged between the extracellular medium and the membrane binding sites without ever fully crossing the membrane. These steps are voltage-dependent with a negative membrane potential favoring binding and occlusion and positive membrane potential favoring de-occlusion and release. Internal ([Na]i) and external Na+ concentration ([Na]0) has also been shown to modulate Na+ translocation in distinct ways (5).

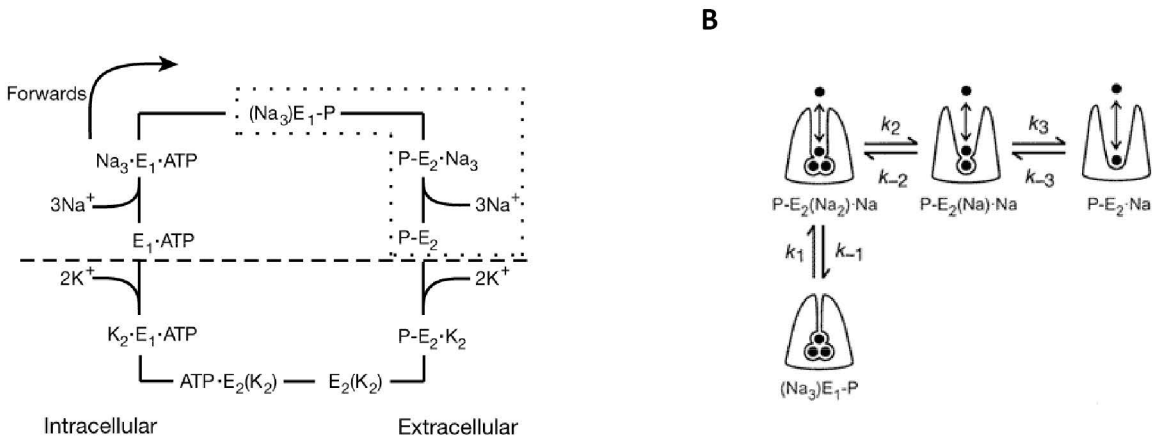

Figure 1 Kinetic models of Na/K Pump activity **A** Post-Albers transport cycle. This cycle contains two major conformations: E1 with binding sites facing cytoplasm and E2 with binding sites facing the extracellular medium. In the cycle two potassium ions are bound from the extracellular medium in the E2 state. Then ATP is bound inducing a conformational change to E1 which releases the potassium ions. Three sodium ions are then bound from the cytoplasm and coupled to a phosphorylation reaction. This reaction drives a conformational change back to E2 which allows the release of sodium ions. Steps inside dashed line represent sodium translocation steps when pumps are deprived of extracellular potassium. **B** Sodium Translocation Model proposed by Holmgren et al, 2000. Electrogenic events are shown as sodium ions traveling through a narrow access channel. Three steps exists representing slow, medium, and fast components of charge. The channel widens from component to component reducing electrogenicity. (Taken from Holmgren et al, 2000)

Previous work has shown that the electrical signals resulting from Na+ translocation are due to ions traversing an access channel that connects Na+ binding sites to the extracellular side of the membrane. This channel has similar properties to the permeation pathway of an ion channel and has been estimated to span approximately 70% of the membrane's electric field (6, 7). Pre-steady-state charge movements may be measured using high-speed voltage jumps to assess the kinetics steps within this pathway. In 2000, Holmgren et al (8) used internally-dialysed giant squid axons to show that Na+ release occurs in three precise sequential steps. These steps are deemed the slow, medium, and fast charge components and are characterized by time constants separated by at least an order of magnitude each (fig. 1b).

The physical interpretation of these kinetic steps is that three Na+ are released from the pump in discrete steps with slightly varying properties. The slow component is accompanied by a rate-limiting, strongly electrogenic conformational change. The medium component is also similarly electrogenic but with considerably faster kinetics. Finally, the fast component is believed to be accompanied by a minor conformational change and appears on the same time scale as the membrane capacitive transient with minimal voltage-dependence. While the general relationships between charge components have been elucidated, precise kinetic properties such as the relaxation rate constants of medium and fast components as well as the relative charge-voltage relationships of the three components are still unknown.

Structurally, the Na/K ATPase consists of an alpha subunit that is always co-expressed with a beta subunit which is primarily involved in membrane localization. An accessory gamma subunit, whose function is largely unknown, has been shown to associate with the pump in specific tissues including the kidney. The alpha subunit

contains ten trans-membrane helices (M1-M10) along with 5 extracellular loops, 4 intracellular loops, and intracellular N and C-terminal tails. The intracellular loops are significantly larger and contain the pump's three primary functional domains: the N, P, and A domains. The N (nucleotide) domain binds ATP, the P (phosphorylation) domain catalyzes a phosphoryl transfer reaction, and the A (actuator) domain contributes to dephosphorylation and coupling of this energy to ion transport (1).

Considerable attention has been paid to the cation binding sites of the Na/K pump in recent years. A consistent model of pump function must incorporate its structural elements and use them to explain functional data, including the precise location of ion binding. In 2002, Ogawa et al (9) published a homology model of the Na/K pump based on the SERCA1A sarcoplasmic calcium pump. In this work, they proposed all five cation binding sites which all are believed to reside within the interior of the membrane via coordination of many transmembrane helices (fig 2a, b). Most notably, Ogawa et al were able to propose a third Na+ binding site despite the lack of an analog in SERCA1A (which only binds two Ca2+). See figure 2c for a summary of the properties of the Na+ binding sites and site-specific mutants developed for the included experiments in this study. The proposal of binding sites for Na+ immediately raised the question of how these sites fit the functional data on Na+ translocation (10).

A

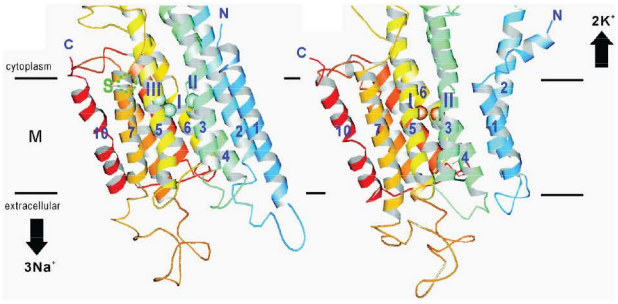

B

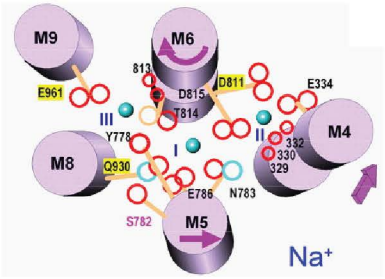

C

	Na^+ Site I	Na^+ Site II	Na^+ Site III
Coordinating Helices	M5,M6,M8	M4, M6	M5,M6,M9
Unique Coordinating Residues	E791D (M5)	E339D (M4)	Y783F (M5)
	N788Q (M5)	D816E (M7)	E966 D (M9)
	Q935N (M8)		
Valence	1.12	0.97	0.96
Distance (Å)	2.42-2.57	2.43-3.03	2.50-2.83

Figure 2 Structural characteristics of the cation binding sites of the Na/K Pump. (from Ref. 9) **A** Model of TM region of the Na/K pump. The E2 conformation is shown on the left with Na+ ions (green) bound. E1 is on the right with K+ ions bound (orange). Site S is a region of valence=0.9. **B** Schematic diagram of Na+ binding sites viewed from the cytoplasmic side. Arrows show motion of TM helices during E1-E2 conformational change. Na+ ions (solid circles) are shown in cyan. Red circles are oxygen atoms; blue are nitrogen, orange are carbon. Yellow residues differ between Na/K pump and SERCA1A. **C** Summary of Na+ binding sites and associated point mutations used in this project.

In 2007, a crystal structure of the sodium-potassium ATPase was published at 3.5 Å resolution with the alpha, beta, and gamma subunits co-crystallized (11). The pump was captured in the E2-P state with two rubidium ions bound as potassium congeners. While this structure doesn't resolve the location of the Na+ binding sites, it does reveal some interesting features. K+ binding sites are remarkably similar to those proposed by the homology models of Ogawa et al. It was also shown that the C-terminal domain (and its conserved KETYY-motif) interacts with the binding pocket and regulates Na+ binding but not K+ binding. This has been proposed to be through interactions with Na+ binding site III which is located in the vicinity of the C-terminal tail in the membrane. Furthermore, it was proposed that a series of basic residues on M10 may be responsible for the pump's voltage dependence and interact with binding sites via the C-terminal domain.

In recent years, the marine toxin palytoxin has been used to probe the Na/K pump in a channel-like state. When added to the system, palytoxin uncouples the intracellular and extracellular gates of the pump, allowing both to be open at the same time under certain conditions (12, 13). This allows the pump to act as a non-specific cation channel that can be measured with single-channel recordings. Using palytoxin, along with modification of engineered cysteine residues by MTS reagents, Reyes et al (14) and Takeuchi et al (15) were able to map the permeation pathway of palytoxin-opened "pump-channels". It was shown that ions enter the pathway extracellularly from a large-vestibule where electrostatic interactions dominate and permeate to a narrower, sterically-controlled region deep in the membrane. A selectivity filter was proposed to be coordinated by four residues in M4 (including Na+ binding site II residue, E339) and M6. Questions still remain about the relation between the pathway of palytoxin-opened pumps and the pathway of the normal coupled pump. However, this work has given some insight into how Na+ is translocated in the pump and where binding sites are positioned relative to the pathway. It was found that residues in M5 believed to coordinate Na+ binding site I were inaccessible to MTS reagents in opened pumps. This was believed to be due to unfavorable geometry because this site does not lie on the principal ion pathway.

Recently, there have also been interesting findings regarding adaptations to various marine environments by the Na/K ATPase. It was found that the squid giant axon-specific form of the pump contains an extracellular ring of positively-charged residues that uses electrostatics to lower local salt concentration and allow the pump to function properly at high external salt concentrations (16). It was also found in the brine shrimp Artemia Franciscana that an isoform of the Na/K ATPase alpha subunit with a double mutation of both residues N324 and N776 to lysine is expressed in response to incubation in environments with high salt concentrations (17). The N776 residue has been shown to be involved in Na+ binding at site I. Homology models show the mutated N776K side chain to plug cation binding site I, potentially wiping out all binding at that site. Further functional studies showed that the mutant N776K had a reduced number of Na+ bound per ATP hydrolyzed and also exhibited significantly decreased Na+ and K+ affinities (18). Physiologically, these mutations are believed to allow the pump to work more efficiently against altered Na+ and K+ gradients. These studies have raised interesting fundamental questions about ion transport in the Na/K pump and show how regulation of cation binding lies at the heart of pump activity.

In this work I have attempted to further elucidate the precise, sequential kinetics of Na+ translocation in the Na/K ATPase. Using the cut-open oocyte vaseline gap (COVG) method (19), I have been able to record pre-steady

state transient currents that reveal further evidence for a sequential model of Na+ release and confirm many findings previously only shown in squid axons. I have obtained charge-voltage curves for slow and medium components from the same oocyte, showing a midpoint shift of 40 mV and a minor decrease in electrogenicity in the medium component. I have also begun to explore the role of Na+ binding sites in Na+ translocation with the goal of determining which binding site produces which component of charge (slow, medium, or fast). Using site-specific mutants, I have accumulated evidence that site III produces the slow component of charge and sites I and II producing medium and fast components respectively. Along with electrophysiological experiments, the integration of various sources of previous structural data is very important for developing a complete picture of the process of Na+ translocation by the Na/K pump and has provided an important perspective on this work.

Methods:

Subcloning, Mutagenesis, and Expression of Na/K pump RNA.

Squid alpha and beta subunits were subcloned into a pBSTA Xenopus high expression vector. The vector contains sequences complementary to the 5' and 3' UTRs of the Xenopus beta-globin mRNA. A consensus eukaryotic translation initiation signal was inserted immediately before the start codon (AUG). Constructs were used to synthesize cRNA using a T7 promoter-based kit. Mutagenesis was performed using standard PCR-based techniques. All mutants were generated using Pfu DNA polymerase and verified by DNA sequencing. Xenopus laevis were maintained and oocytes were isolated using standard techniques. Oocytes were incubated in ND96 solution. Alpha and beta Na/K pump cRNAs were mixed in a 3:1 mass ratio to reflect the relative masses of the two subunits and their 1:1 stoichiometry. A total of 50.6 ng of cRNA were injected into each oocyte. Experiments were done 3-5 days after injection.

Electrophysiology.

Na+ translocation was measured using the cut-open oocyte techniques (19), with sampling exclusively from the animal pole of the oocyte. Membrane potential was clamped using a Dagan CA-1B High Performance Oocyte Clamp. A Tektronix TDS 2012 Two Channel Digital Storage Oscilloscope was used along with Clampex 9 software to control voltage protocols and digitize analog signals. Signals were acquired at 100 kHz and filtered at 20 kHz. Intracellular voltage was measured with a 0.1-0.5 MΩ glass pipette filled with 1 M NaCl. Bridges were filled with 3 M sodium-MES buffer in 3% agarose and contained platinum wires to make electrical connections. Oocyte vegetal poles were permeabilized with 0.1% saponin in internal solution. Time controls were used to assess the stability of the oocyte. Current sensitive to 100 µM extracellular ouabain was deemed pump-mediated. The extracellular solution was (in mM) 110 Na-Glutamate, 5 $BaCl_2$, 2 $NiCl_2$, 5 Hepes, 2 $MgCl_2$, and 0.3 Niflumic Acid (pH=7.6). The intracellular solution was (in mM) 80 Na-Glutamate, 20 TEA-OH (20%), 10 $MgSO_4$, 5 EGTA, 10 Hepes, and 5 ATP-Mg (pH=7.3).

Data Analysis.

Data was analyzed with Clampfit 9.2 and Origin 8 software. Data was filtered (if necessary) using an 8-pole Bessel low-pass filter. Relaxation rates were obtained from the inverse of one and two component exponential fits to the ON (during voltage step) current traces for genomic and mutant pumps. Relaxation Rate-Voltage curves were fit

using the modified Hill equation as previously described (8). The amount of charge translocated was determined either by using direct integration of currents or through one or two component exponential fits of the OFF (after voltage step) current. Error bars represent values from error propagation on fit data and thus represent how well the data points fit the function used for their determination. Figure 12 was produced using PyMol (www.pymol.org).

Results:

In order to assess Na+ translocation kinetics in genomic pumps, various voltage protocols were performed. Figure 3 shows the general protocol for acquiring pump-mediated charge translocation. The pump was deprived of external K+ and provided internal ATP in order to trap it in Na+ translocation steps (Fig. 1). In this long pulse (30 ms, -70 mV) two components may be seen in both the ON and OFF currents. Negative membrane potential electrostatically favors the approach of Na+ to the membrane where they may bind the Na/K pump. This provides the basis for the interpretation of Na+ translocation currents. In the ON current, a fast component reflecting electrogenic Na+ binding is followed by a slow component reflecting Na+ occlusion and the associated E2→E1 conformational change. Accordingly, the OFF current contains a slow component reflecting Na+ de-occlusion (E1→E2 conformational change) and a fast component reflecting electrogenic Na+ release.

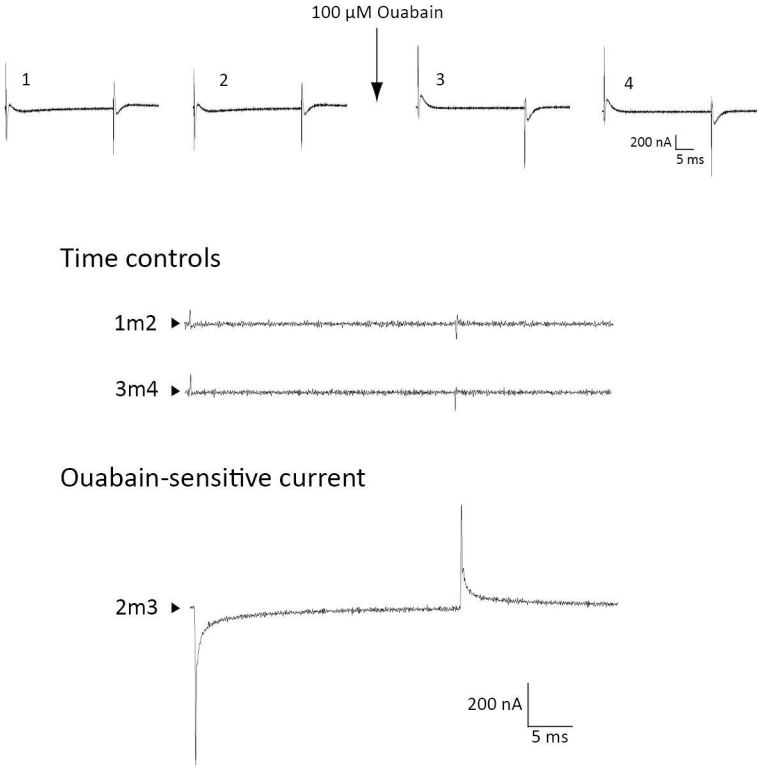

Figure 3 Charge movement during sodium translocation by the Na/K pump. The method for determination of pump-mediated current is shown. Traces 1-4 show averages of 4 current responses to 30-ms voltage jumps from 0 to -70 mV. Traces 1 and 2 were before and traces 3 and 4 were after extracellular application of 100 µM of the Na/K pump blocker ouabain. Difference currents 1-2 and 3-4 show stability of cut-open system over time. Difference current 2-3 shows pump-mediated charge translocation. ON and OFF currents may be fit with two-exponential functions yielding τ values of 0.15 and 5 ms (ON) and 0.2 and 4.4 ms (OFF). The function used was:

$y = y0 + A1*\exp(-(x-x0)/t1) + A2*\exp(-(x-x0)/t2)$.

Data was acquired at 100 kHz and filtered at 5 kHz. Arrowheads mark zero current point.

In order to provide further evidence for the above interpretation of Na+ translocation currents, various protocols were performed to determine the sequential character of binding and occlusion steps. Results, found for the first time in Xenopus oocytes, were consistent with previous experiments in squid axons (ref. 8). In figure 4a, the membrane was clamped to a very negative potential (-130 mV) for 20 ms. In response, current traces show fast (binding) and slow (occlusion) components in the ON current that completely relax to 0 nA, with a loss of the fast component upon relaxation to 0 mV. This is interpreted as a result of longer, negative pulses favoring Na/K pumps occupying the occluded (Na3) E1-P state and being unable to immediately release Na+ upon the jump back to 0 mV. In the second pulse in figure 4a, the opposite experiment is run. The membrane is clamped to a positive potential (+80 mV) for 30 ms. Fast and slow components of outward current are seen during the ON current. However, when the voltage jumps back to 0 mV, there is a significant increase in the amount of fast charge translocated. This is interpreted as a result of positive potentials favoring Na+ release which maximizes the number of pumps able to bind Na+ when the potential is dropped back to 0 mV. This increased binding ability manifests itself in an enhanced inward fast-component of charge.

To resolve any additional charge components, briefer pulse protocols were applied to genomic Na/K pumps. In figure 4b a 1.5 ms, -190 mV pulse prevents current relaxation to the steady state (0 nA; dotted line). Interestingly, when the potential is jumped back to zero, this allows for the detection of a medium charge component. This component has a time constant that is an order of magnitude faster than the slow component, but an order of magnitude slower than the fast component. This result confirms findings by Holmgren et al (8) that led to the three component model proposed (fig. 1b). The medium component's presence greatly supports the concept that Na+ is bound/occluded and de-occluded/released sequentially through a high-energy access channel that exists between occlusion/de-occlusion transitions. The medium component is not detected in longer pulses because it is dominated (in magnitude) by the slow and fast charges. However, when slow charge saturation is prevented by using shorter pulses it can be clearly resolved and studied in the OFF current.

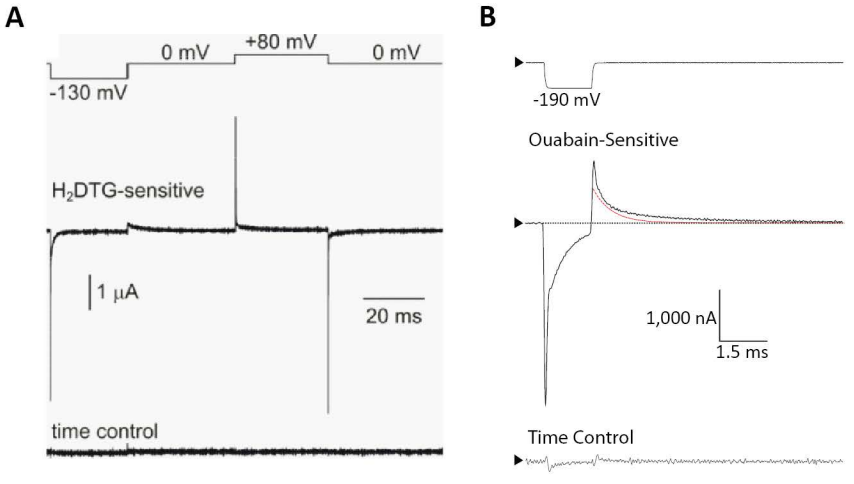

Figure 4 Components of charge appear in sequence **A** Fast and slow components occur sequentially. In the first voltage pulse, as a result of a negative membrane potential for 30 ms, fast charge immobilization is seen in the OFF current. The ON current contains fast (τ≈0.05 ms) and slow charge (τ≈6 ms). The OFF current, due to immobilization of pumps in the (Na3) E1-P state, only contains a slow component (τ≈6 ms). In the second pulse a prolonged positive potential produces enhanced fast charge in the OFF current. This is due to an increased proportion available pumps in the P-E2 state with no sodium ions bound. **B** Medium charge component appears in shorter pulse protocols. A voltage pulse to -190 mV for 1.5 ms prevents pump-mediated current relaxation to 0 nA (steady state). Upon the jump to 0 mV, a medium component (red) is revealed with a time constant (τ≈0.6 ms) intermediate to slow and fast components.

Using long pulse protocols, charge-voltage and relaxation rate constant (K)- voltage curves were produced for the genomic Na/K pump (fig. 5). As previously shown, the relaxation rate constant of the slow component between -140 and 40 mV with 110 mM [Na]0 ranges from 600 Hz (for negative potentials) to just below 200 Hz (for positive potentials). As the membrane potential gets more negative the rate of the slow component of Na+ translocation increases until it begins to saturate at around -150 mV. On the other end, positive potentials do not elicit any change in the relaxation rate constant (K) and the plot shows an approximately flat line between -20 to 40 mV. This data was fit with a modified Hill equation which revealed, most notably, a value for λ (the fraction of the membrane's electric field crossed by the access channel) of 0.72 which is consistent with several previous findings (ref. 4, 7, 8). Ultimately, it is shown that at large negative membrane potentials and positive membrane potentials the rate of occlusion/deocclusion is relatively electroneutral. However, in the region in between these extremes, K is modulated by both voltage and [Na]0.

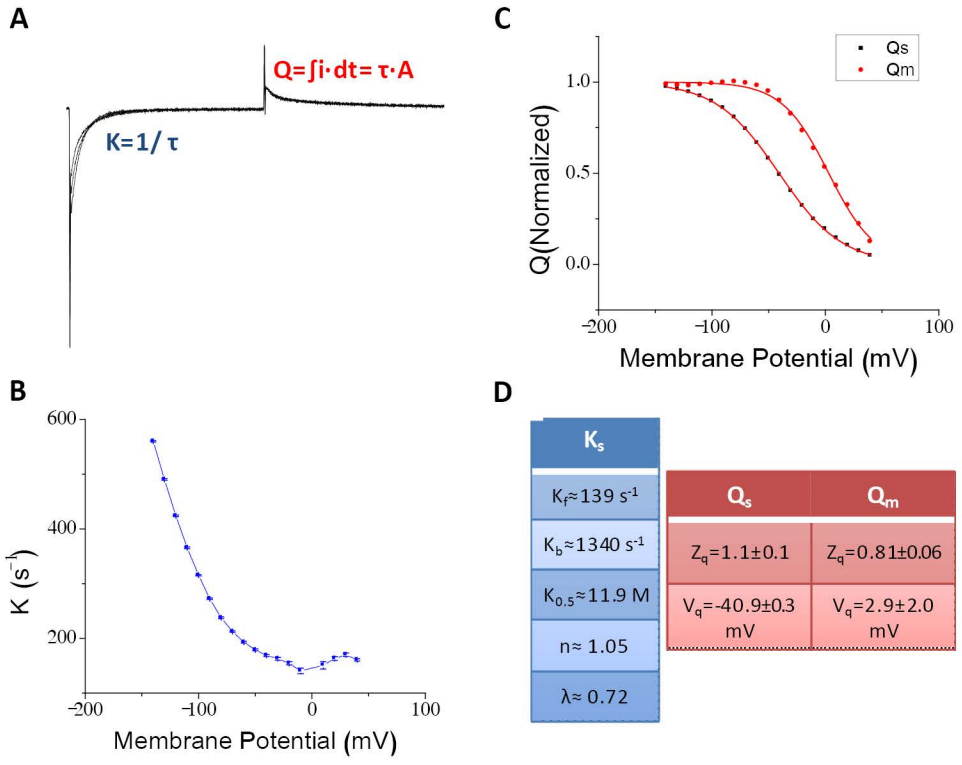

Figure 5 Characterization of Na+ translocation in genomic Na/K pumps at 110 mM [Na]0. **A** Method for determining the amount of charge translocated and relaxation rate constant for Na/K pumps. The relaxation rate constant (K) may be determined by fitting the ON current with an exponential function and using the shown equation (red) to convert the time constant (τ) into K. To determine charge translocated (Q), the OFF current can either be integrated or time constants and amplitudes of exponential fits may be used to determine a value. **B** K for different values of membrane potential. Data is fit with a modified Hill equation (shown) where kf and kb are voltage-independent forward and backward rate constants, K0.5 is the half-activating [Na] at 0 mV, n is the Hill coefficient, and λ is the fraction of the membrane's electric field dropped over access channel. **C** Charge-voltage curves for the slow (Qs) and medium (Qm) components of charge. Data is fit with a Boltzmann function and normalized using the equation shown. **D** Summary of values obtained from fitting K-V and Q-V curves.

Charge-voltage curves were obtained for both the medium and slow components of charge from genomic Na/K pumps. Both curves were fit with Boltzmann equations (Fig. 5c) which revealed the relative voltage-dependence of each component. It was found that the slow component of charge has a midpoint (Vq) at -40.9 mV as compared to the medium component which has a midpoint that is shifted to the right by 44 mV to 2.9 mV. This indicates that charge saturation occurs at less negative voltages for the medium component. This is predicted by the 3 step model of Holmgren et al, but the medium and slow components had yet to be shown together in the same recording in this way. Furthermore, the apparent valence (zq) of the Q-V curves is slightly decreased in the medium component from 1.1 to 0.81. This indicates a slightly less steep voltage-dependence for the medium component due to a widened, less-focused access channel. Values for the midpoint (-40.9 mV) and apparent valence (1.1) of the slow component are very similar to previous findings (-43 mV, 1) in exogenous squid Na/K pumps in oocytes (see Ref. 16).

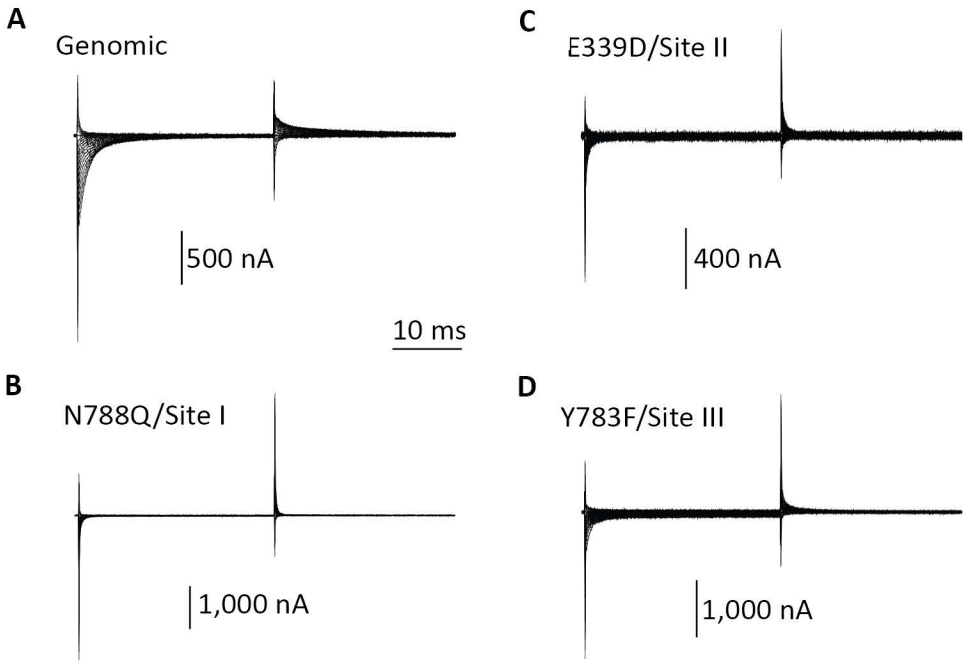

Figure 6 Current traces in response to 30 ms voltage steps from -140 mV to 60 mV in 10 mV increments. Data was acquired at 100 kHz. Mutants show distinct qualitative phenotypes. **A** Genomic pumps are characterized by pronounced slow components in both the ON and OFF. Also, there is significant immobilzation of fast charge in the OFF due to the long duration of the pulse. **B** N788Q/Site I and **C** E339D/Site II both display significantly faster rates of current decay in both ON and OFF as compared to the genomic. There is no evidence for immobilization of fast charge in either. **D** Y783F/Site III also shows faster kinetics, however, there is still a pronounced slow component which is especially visible in the ON current. This component appears to have rates similar to the slow component observed in the genomic pump.

Na+ binding sites were analyzed. Mutations were made to residues that contribute side chain interactions that are specific to only one of the three proposed Na+ binding sites. Furthermore mutations preserved the general character of the amino acid. Mutations were between tyrosine (Y) and phenylalanine (F), aspartate (D) and glutamate (E), and asparagine (N) and glutamine (Q) (fig. 2c). Figure 6 shows representative current traces for mutations to site I (N788Q), site II (E339D), and site III (Y783F), as well as the genomic Na/K pump, in response to 30 ms voltage pulses ranging from -140 mV to 40 mV in increments of 10 mV. In the genomic Na/K pumps (Fig. 6a) there is clear immobilization of the fast charge in the OFF current that is more pronounced as the voltage decreases. There are clear slow and fast components of the ON charge as well, which have been shown in previous experiments. However, in the site I and site II mutants N788Q and E339D, the ON and OFF currents are essentially symmetrical

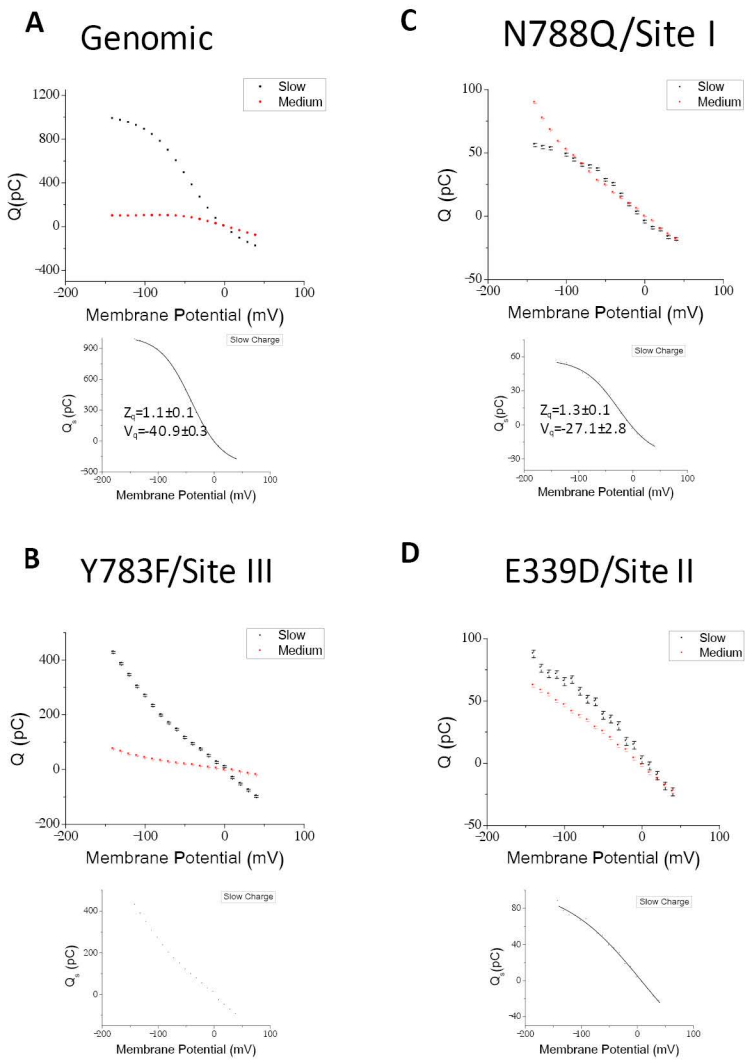

Figure 7 Charge-Voltage curves for slow and medium components of charge for genomic and sodium binding site mutant Na/K pumps. In **A** Genomic and **B** Y783F/site III slow charge (black)amplitude is much larger than medium charge (red). However, in **C** N788Q/site I and **D** E339D/site II the slow charge is of a comparable amplitude to the medium charge indicating the relative absence of slow charge translocation. Curves were obtained by fitting OFF currents with two component exponentials with fixed time constants. Time constants were (in ms): genomic-12 and 1.4, Y783F-3.3 and 0.3, N788Q-3.5 and 0.3, E339D-3 and 0.5. Slow charge-voltage relationships are shown below each slow/medium plot by itself with Boltzmann fit parameters.

Relaxation rate constant (K) values were also determined for the various mutants. This analysis is complied in figure 8. For Y783F (fig. 8b), the ON current was fit with a one component exponential that corresponded to the slow component of charge. This conclusion was based on the time constant and the charge-voltage curve analysis which showed the presence of significant slow component. The K-voltage curve for Y783F shows a similar magnitude to the K-voltage curve for genomic pumps (fig. 8a) but with some altered properties. K increases much less rapidly as voltage decreases compared to the genomic. Also, voltages greater than -20 mV do not result in a flattened curve for K; rather, there is a clear increase in K as voltage increases in this region. This represents some shift in the voltage dependence of K as a result of this mutation. This “V” shaped curve is seen in all three of the mutants and does not lend itself to a simple interpretation.

In the N788Q mutant pump current the ON trace could not be successfully fit with just one component. Instead, it was fit with two components which corresponded to medium and fast components respectively. In figure 8c, the K values for the medium component were plotted in isolation for comparison with the other mutants. For E339D (fig. 8d), the ON current was fit with one component that corresponded to the medium component of charge. This resulted in a K-voltage curve of a similar magnitude to the curve for N788Q. Both curves had values

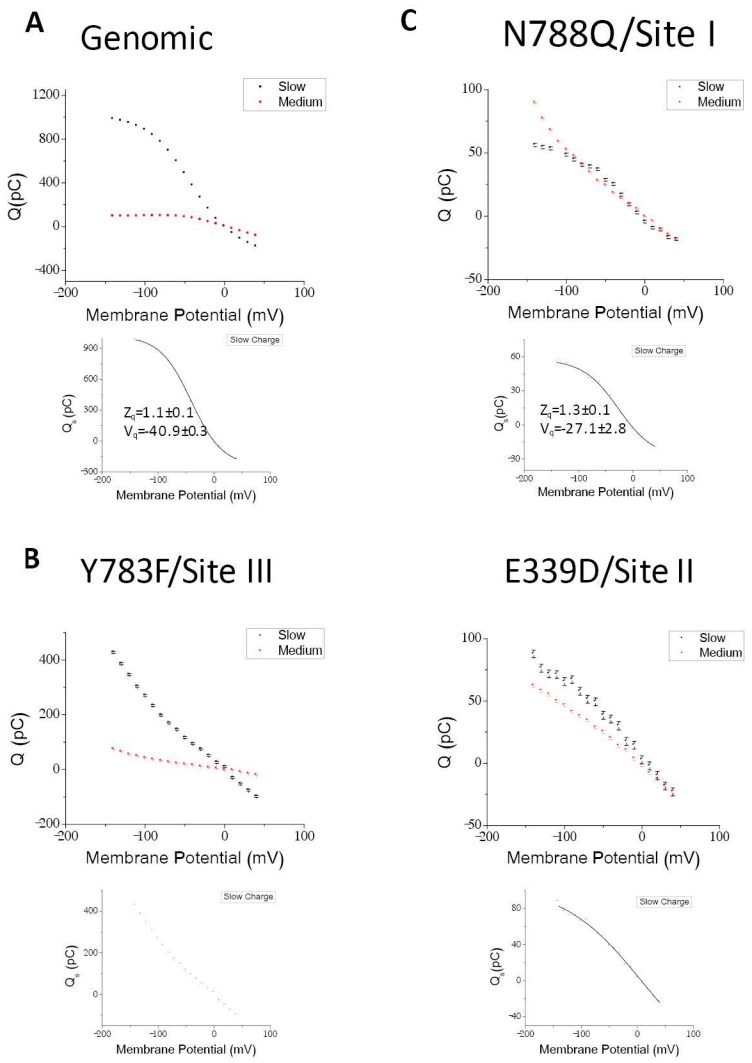

Figure 7 Charge-Voltage curves for slow and medium components of charge for genomic and sodium binding site mutant Na/K pumps. In **A** Genomic and **B** Y783F/site III slow charge (black)amplitude is much larger than medium charge (red). However, in **C** N788Q/site I and **D** E339D/site II the slow charge is of a comparable amplitude to the medium charge indicating the relative absence of slow charge translocation. Curves were obtained by fitting OFF currents with two component exponentials with fixed time constants. Time constants were (in ms): genomic-12 and 1.4, Y783F-3.3 and 0.3, N788Q-3.5 and 0.3, E339D-3 and 0.5. Slow charge-voltage relationships are shown below each slow/medium plot by itself with Boltzmann fit parameters.

Relaxation rate constant (K) values were also determined for the various mutants. This analysis is complied in figure 8. For Y783F (fig. 8b), the ON current was fit with a one component exponential that corresponded to the slow component of charge. This conclusion was based on the time constant and the charge-voltage curve analysis which showed the presence of significant slow component. The K-voltage curve for Y783F shows a similar magnitude to the K-voltage curve for genomic pumps (fig. 8a) but with some altered properties. K increases much less rapidly as voltage decreases compared to the genomic. Also, voltages greater than -20 mV do not result in a flattened curve for K; rather, there is a clear increase in K as voltage increases in this region. This represents some shift in the voltage dependence of K as a result of this mutation. This "V" shaped curve is seen in all three of the mutants and does not lend itself to a simple interpretation.

In the N788Q mutant pump current the ON trace could not be successfully fit with just one component. Instead, it was fit with two components which corresponded to medium and fast components respectively. In figure 8c, the K values for the medium component were plotted in isolation for comparison with the other mutants. For E339D (fig. 8d), the ON current was fit with one component that corresponded to the medium component of charge. This resulted in a K-voltage curve of a similar magnitude to the curve for N788Q. Both curves had values

for K ranging from 1200 to 2000 s-1 with the average value appearing to be slightly greater for the E339D/site II mutant. One noticeable difference is that in the N788Q plot there appears to be some saturation at very negative voltages (>-120 mV) which is not seen in E339D. Perhaps the medium component's relaxation rate constant curve is slightly shifted to the right in N788Q relative to E339D. Further experiments will need to be performed to determine the validity of this hypothesis.

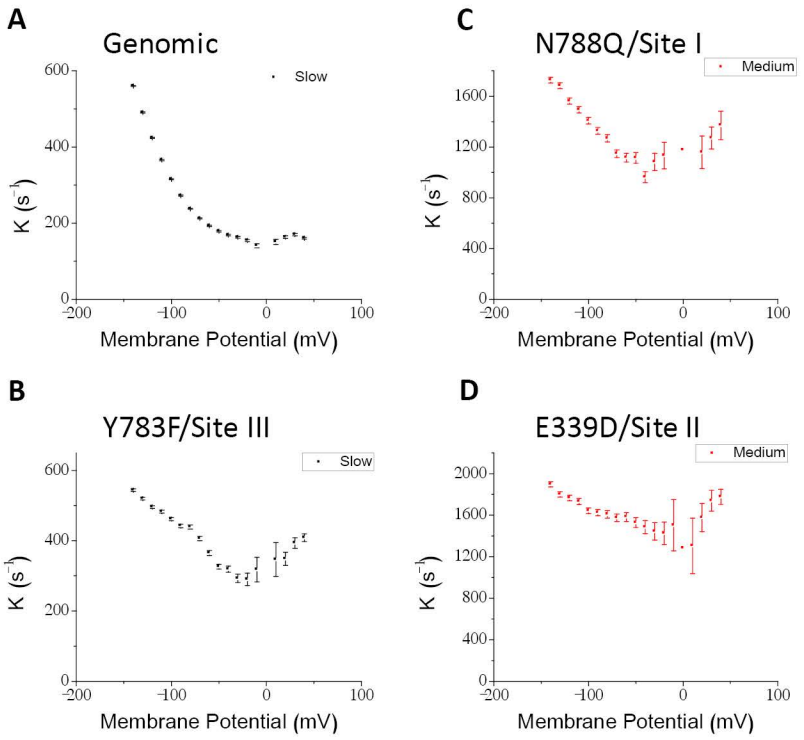

Figure 8 Relaxation Rate Constant (K)-Voltage curves for slow and medium components of charge for genomic and sodium binding site mutant Na/K pumps. In **A** Genomic and **B** Y783F/site III ON currents were fit with one component producing K values for the slow charge component. In **C** N788Q/site I and **D** E339D/site II results of one component exponential fits were interpreted as values for the medium charge component. Error bars were determined using error propagation based on error values for time constants of exponential fits.

In N788Q/site I mutants, due to the high quality of recordings relative to the other mutants, two components of current were extracted from the ON traces. This resulted in K-V curves for the medium and fast components (Fig. 9); slow charge was deemed to not be present in this mutant. Interestingly, the fast K values range as high as 12,000 s-1 and show clear saturation at negative voltages. This may offer some clue for what the K-voltage curve for the genomic medium and fast components look like as well as offering clues for what component of charge is produced by Na+ binding site I.

While charge-voltage and K-voltage curves for the medium and slow component of charge offer a look at the relative kinetics of the transitions in the genomic Na/K pump, it is also necessary to understand the duration dependence of each charge component. Duration dependence means the relative amount of charge moved by each component as a function of the length of a voltage pulse at a fixed membrane potential. This is tested in the following experiments where all pulses were to -190 mV for durations ranging from 100 µs to 4 ms. Most of these pulses do not provide enough time for the pump to reach a steady state and thus, allowed the resolution of all three components of charge. The 3-step kinetic model proposed makes clear predictions about the behavior of all three charge components in such experiments. It is believed that with increased pulse length the magnitude of the fast component of charge will decrease while the slow component will increase. Accordingly the medium compo-

nent of charge will see two periods of duration-dependence. At short durations the medium component is expected to grow as more pumps are driven back toward the P-E2(Na2) state and allow the medium component to be seen on relaxation. Inversely, beyond a certain point as the pulse duration increases it is believed that more pumps will occupy the P-E2(Na3) state mobilizing the slow component of charge. This slow charge mobilization will lead to medium charge immobilization (as is also predicted for the fast component) and a subsequent decrease in the amount of slow charge translocated.

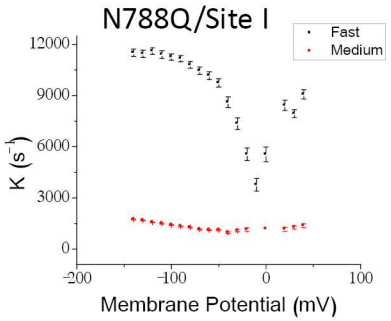

Figure 9 Relaxation Rate Constant (K)-Voltage curves for the fast and medium components of charge in the N788Q/site I mutant. Values for K were obtained using two component exponential fits to the ON current.

These predictions are all fulfilled in the experimental results presented in figure 10. Fast charge, assayed as the maximum current amplitude in the OFF trace, decreases exponentially with pulse duration. The slow component also increases exponentially with duration as expected. Finally, the medium component rises to peak amplitude around 1-1.5 ms followed by an exponential decrease as duration increases. This data may be fit with the difference of two exponentials where the decay matches the time constant of the slow component of the ON current. Furthermore, this time constant matches that of the slow charge component, indicating that the medium charge decays proportionally as the slow grows. Ultimately, this experiment shows the sequential nature of the three charge components by the fact that they grow and shrink at the expense of each other. Furthermore, the amplitudes of the charge components are consistent with results found in voltage-sensitivity analysis (fig. 7). The magnitude of the slow charge is almost always greater than the medium charge and as the pulse duration increases this discrepancy widens to a point where Qs is twice as large as Qm. Also, the fast component, here indirectly measured as total current amplitude, were it to be multiplied by its estimated time constant (0.03 ms) would be significantly smaller than the medium and slow components as predicted.

If the duration-dependence of charge components shows their discrete, sequential nature, mutations specific to Na+ binding site should show some alterations to the relationships of each component with pulse duration. This is a useful way to find clues as to which binding site produces which component of charge during Na+ translocation. These experiments have produced interesting results in the site I mutant N788Q, as well as the site III mutant E966D. These results are compiled in figure 11.

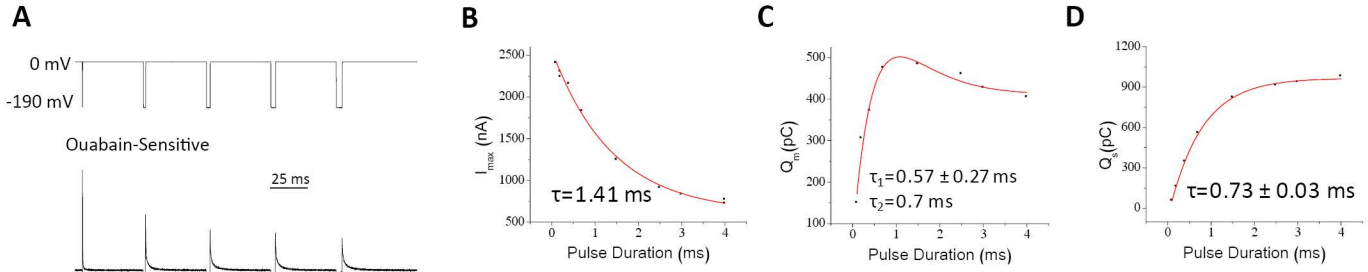

Figure 10 Three components of charge grow at the expense of each other as pulse duration increases. **A** Representative current traces for genomic Na/K pumps in response to -190 mV pulses of varying durations (0.1, 0.2, 0.4, 0.7, 4 ms). **B** Maximum amplitude of OFF current for varying pulse durations. This is viewed as an assay of how fast charge changes with duration. **C** Medium charge versus pulse duration. Data is fit with a difference of two exponentials. **D** Growth of slow charge as duration increases. Slow and medium charge values were determined by fitting each OFF current with a 3-component exponential. Data is representative; time constants for charge-duration plots are averages of 3 experiments.

While the maximum current amplitude of the OFF trace may be a useful measure of fast charge, it should also be noted that is far more subject to error due to data subtraction issues than the other three components. For this reason, noise in the Imax-Duration plots is expected and interpretation of data should focus on slow and medium components. In the N788Q/site I mutant, greatly decreased slow charge amplitude is seen as expected based on charge-voltage curves (fig. 11c). However, slow charge grows with pulse duration as expected for endogenous pumps. More interestingly, the medium component does not show any immobilization with increase in charge duration (fig. 11b). Instead, the plot may be fit with a one component exponential with time constant slightly slower than the medium charge-duration plot growth time constant for the genomic Na/K pump. This is consistent with the idea of slow binding being prevented from occurring in site I mutants, thus causing the medium charge to saturate as the slow charge would be expected to.

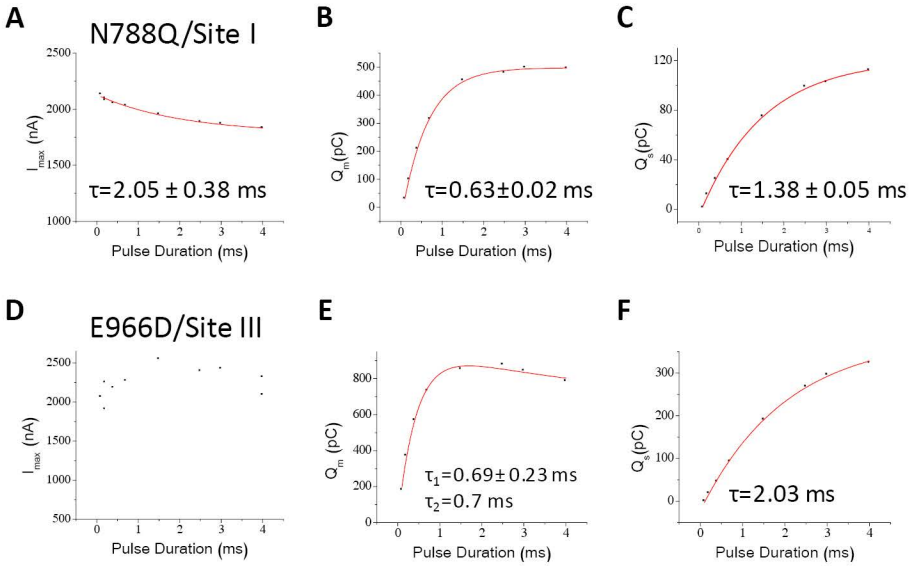

Figure 11 Three components of pump-mediated charge are altered in Na+ binding site I (top traces) and site III (bottom traces) mutants. Pulse duration-dependence on **A** fast (assayed as Imax at OFF), **B** medium, and **C** slow components of charge in N788Q/site I mutants. The same plots are shown for E966D /site III mutant in **D** fast, **E** medium, and **F** slow. All pulses were to -190 mV and charge values were obtained in the same way as for genomic Na/K pumps in fig. 10. Plots are representative while time constants are averages of 2 or more experiments.

In the E966D/site III mutant a different phenotype is seen. The slow component is seen with much larger amplitude than the site I or site II mutants (not shown) but with significantly slower time constant of growth as pulse duration increases (fig. 11f). Furthermore, the medium component of charge still exhibits two phases as pulse duration increases: a growth phase followed by a decay phase (fig. 11e). However, the decay phase is shifted to greater duration and is less pronounced. The peak of the exponential fit is around 2.5 ms as opposed to 1 ms for the genomic pumps. This indicates that exogenous slow charge is being translocated but that its amplitude is growing more slowly and subsequently immobilizing medium charge less effectively. This is consistent with the interpretation of site III as producing the slow component of charge and will be explored in the discussion. Similar experiments were performed with other mutants (Q935N/site I, E339D/site II, D816E/site II) but due to low expression and difficulty in fitting data, results have not been shown.

Discussion:

The cut-open oocyte voltage clamp system allows for rapid voltage steps and data acquisition in exogenously expressed Na/K pumps. This property has been used in the described experiments to assess the kinetics and underlying structural changes during Na+ translocation by the Na/K pump. Notably, experiments performed on genomic pumps in this project confirm previous findings in the squid giant axon performed over the last 10 years (4-8). Also, further evidence for a three-step sequential model of Na+ release has been compiled. Charge-voltage curves for the slow and medium components from the same oocyte (i.e. the same ensemble of pumps during the same protocol) show the relative voltage sensitivity of the two components (fig. 5c). The medium component is shifted to the right and begins to saturate at much less negative membrane potential. It also has a slightly decreased apparent valence indicating similar, but less steep, voltage dependence as compared to the slow component. This may be explained using the access channel model. During the medium transition the membrane's electric field is less focused than during the slow transition and thus medium charge is less voltage-dependent.

Experiments measuring the dependence of each charge component on the duration of a negative voltage pulse showed further evidence for the sequential model. Fast charge was seen to immobilize while slow charge grows with pulse duration. Most strikingly, the medium component shows a growth phase followed by a decay phase where it is immobilized by the slow component. These experiments confirm that the slow, medium, and fast components of charge grow at the expense of the previous component and thus, occur in a precise sequence.

With a sequential model for the translocation of Na+ by the Na/K pump, it is important to reconcile this kinetic perspective with a structural one. Using data from homology models, mutations were made to various residues proposed to contribute to Na+ binding sites I, II, and III. These mutations showed very drastic changes as compared to the genomic pumps under various voltage protocols. Prior to any quantitative analysis of these results, it is worth noting that each mutation's result is indicative of the role of each residue in Na+ binding and is a useful crosschecks for the results of homology modeling. On a deeper level, these mutations have provided some evidence that will lead to the development of a full model of which binding site produces which component of charge. The following discussion is based on limited experiments performed so far and as such is preliminary, but will be

useful in designing future experiments to test predictions.

There appears to be a series of reasons why site III is likely to produce the slow component of charge. Regardless of experiments, it is intuitive to think that the binding site that is unique to Na+ (unlike sites I and II) would produce the major step in the E2-E1 conformational change. This is especially suggestive because K+ translocation does not produce a slow component. In experiments using long pulses to various voltages, there was significant evidence for the presence of a slow component of charge in site III mutants Y783F (fig. 6d) and E966D (data not shown). Charge-voltage plots show that a majority of charge translocation comes from the slow component which is similar to the genomic Na/K pump (Fig. 7a,b). In contrast, the site I and site II mutants do not show any slow component that may be distinguished from endogenous pumps. In Q-V curves for Y783F mutants, the voltage-dependence is very altered, however, indicating that there are large changes occurring to the slow transition during Na+ translocation. Furthermore, relaxation rate constants for Y783F are similar to those for the slow component in genomic pumps, despite decreased voltage-sensitivity.

Overall, these results indicate that the site III mutants exhibit slow charge due to alteration of the specific binding site that releases the slow component. In the site I and site II mutants, presumably, mutations are affecting binding of either fast or medium components and preventing progression to the slow site at all. This is confirmed in pulse-duration studies which show a decreased growth of the slow component and a subsequent decrease in medium charge immobilization in the E966D/site III mutant.

One final piece of evidence for the slow component of charge binding and being released from site III is the proximity of site III to the C-terminal tail of the alpha subunit in the crystal structure of the Na/K pump (ref. 11). This tail was shown to contain a YY-motif that enters the trans-membrane region near Na+ binding site III. This tail, when truncated to remove the two tyrosine residues, affects Na+ binding affinity. Furthermore, interaction between the tail and binding site III may be important for determining pump voltage-sensitivity. This is believed because of a series of polar residues on TM 10 that may act in a similar way to the S4 segment of voltage sensing domains in ion channels. Interaction between site III and M10 may be mediated by the C-terminal tail and thus lead to the voltage-sensitivity of Na+ translocation. This is consistent with site III producing the slow component because the slow component is the major voltage-dependent step in Na/K pump function. Modulation of the slow component, here by the C-terminal tail, should result in a shift in voltage-dependence of Na+ translocation as proposed by Morth et al (12).

If site III may be deemed to provide binding and release for the slow component of charge, it is now necessary to resolve between site I and site II which sites produce the fast and medium components. Both sites show near abolition of slow charge movement in mutants N788Q/site I and E339/site II. However, there are some subtle differences between the two phenotypes that provide some clues. The relaxation rate constants were somewhat different between the two mutants. N788Q/site I was able to be fit with exponentials to produce what were deemed medium and a fast K-voltage curves while the E339D/site II mutant was only fit with one exponential to get a medium K-voltage curve. The respective K-voltage curves of the medium components had similar amplitudes although there appeared to be more voltage sensitivity in N788Q. This is believed because of the steeper changes

in K as membrane potential decreases. Furthermore, the K-V for the fast component obtained from N788Q is consistent, based on amplitude, with predictions for the fast component in genomic pumps. This indicates that perhaps the fast component is unaltered in N788Q making site I a potential candidate for the medium component.

Pulse duration-dependence was not assayed in E339D or D816E due to insufficient pump expression. However, in N788Q a phenotype consistent with specific alteration of the medium component was found. The slow charge versus duration plot shows very small amplitude that is believed to be due to endogenous pumps. However, the medium component does not become immobilized and has a similar growth rate to the slow component of genomic pumps. This indicates that the slow component is absent and unable to cause decay in the medium charge.

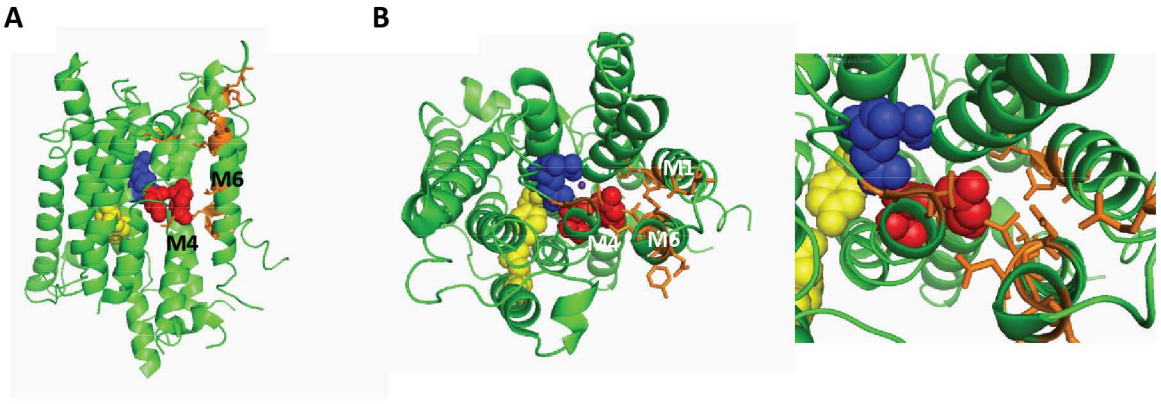

Figure 12 Na+ binding site II lies directly on the permeation pathway of palytoxin-opened Na/K pump. Crystal structure of transmembrane region of Na/K pump alpha subunit in E2P conformation with two rubidium ions (purple) bound as K+ congeners (Morth et al, 2007). Residues specific to Na+ binding sites I (N788, Q935, E791; blue), II (E339, D816; yellow), and III (Y783, E966; red) are shown as spheres. Side chains shown to lie on the permeation pathway of palytoxin-opened channels are shown as sticks in orange. Pump is shown from **A** cross section of membrane and **B** extracellular side of the membrane at two different magnifications. While this structure is in a different conformation than E1 when Na+ is bound and occluded, it still shows a clear pathway primarily between M4, M1, and M6 that implicates site II as responsible for the fast component of charge.

Finally, it is worth looking at the structure of the trans-membrane regions of the pump alpha subunit in relation to the Na+ binding sites and the permeation pathway proposed for palytoxin-opened pump-channels (ref. 14, 15). This is done in figure 12. Unfortunately, the crystal structure is in the E2P conformation with two rubidium ions bound as potassium congeners. However, it is still interesting that the pathway, located primarily between M4 and M6, appears to interact directly with Na+ binding site II. Questions still remain about the relation of the palytoxin-opened path to the native access channel, but these results provide evidence for site II producing the fast component of charge. This is because a site that is directly on the ion pathway would probably be able to bind Na+ at a faster rate than the increasingly peripheral sites I and III. The mechanism by which ions reach site I and site III is puzzling given the pathway in fig. 12 because they appear to reside off of the major permeation pathway. Further structural models, in the E1 conformation particularly, will lead to a clarification of where Na+ ions travel through the transmembrane helices to reach their binding sites.

Overall, this work provides support for a sequential model of Na+ translocation and provides some useful evidence for how each binding site produces the slow, medium, and fast components of charge. Further work will

examine more site-specific mutants and more varying voltage protocols in order to confirm and extend the work presented here. The Na/K pump is an absolutely vital membrane protein for many physiological processes and many interesting questions still remain about its fundamental structure and function.

References:

1. Kaplan, J. 2002. Biochemistry of Na,K-ATPase. Annu. Rev. Biochem. 71: 511-535/
2. Jorgensen, P. et al. 2003. Structure and Mechanism of Na,K-ATPase: Functional Sites and Their Interactions. Annu. Rev. Physiol. 65: 817-849.
3. Nakao, M. et al. 1986. Voltage Dependence of Na Translocation by the Na/K Pump. Nature. 323: 628-630.
4. Holmgren, M. et al. 1994. Pre-Steady-State Transient Currents Mediated by the Na/K Pump in Internally Perfused Xenopus Oocytes. Biophysical Journal. 66: 912-922.
5. Holmgren, M. et al. 2006. Charge Translocation by the Na/K Pump under Na/Na Exchange Conditions: Intracellu lar Na Dependence. Biophysical Journal. 90:1607-1616.
6. Gadsby, D. et al. 1993 Extracellular Access to the Na,K Pump: Pathway Similar to an Ion Channel. Science. 260: 100-103.
7. Sagar, A. et al. 1994. Access Channel Model for the Voltage Dependence of the Forward-Running Na/K pump. Journal of Gen. Phys. 103: 869-893.
8. Holmgren, M. et al. 2000. Three Distinct and Sequential Steps in the Release of Sodium Ions by the Na/K-ATPase. Nature. 403: 898-901.
9. Ogawa, H. et al. 2002. Homology Modeling of the Cation Binding Sites of Na+K+-ATPase. PNAS. 99: 15977-15982.
10. Rakowski, R. et al. 2003. Found: Na and K Binding Sites of the Sodium Pump. News Physiol Sci. 18: 164-168.
11. Morth, J. et al. 2007. Crystal Structure of the Sodium-Potassium Pump. Nature. 450: 1043-1049.
12. Artigas, P. et al. 2003. Na/K Pump Ligands Modulate Gating of Palytoxin-Induced Ion Channels. PNAS. 21: 501-505.
13. Rakowski,R. et al. 2007. Sodium Flux Ratio in Na/K Pump-Channels Opened by Palytoxin. Journal of Gen. Phys. 130: 41-54.
14. Reyes, N. et al. 2006. Ion Permeation Through the Na,K-ATPase. Nature. 443: 470-474.
15. Takeuchi, A. et al. 2008. The Ion Pathway Through the Opened Na,K-ATPase Pump. Nature. 456. 413-416.
16. Colina,C. et al. 2007. Structural Basis of Na/K ATPase Adaptation to Marine Environments. Nature Structural and Molecular Biology. 14: 427-431.
17. Jorgensen, P. et al. 2008. Regulation and Function of Lysine-Substituted Na,K Pumps in Salt Adaptation of Ar temia Francsicana. J. Membrane Biology. 221:39-49.
18. Jorgensen, P. 2008. Importance for Absorption of Na from Freshwater of Lysine, Valine, and Serine Substitutions in the alpha1a-Isoform of Na,K-ATPase in the Gills of Rainbow Trout and Atlantic Salmon. J. Membrane Biol ogy. 223: 37-47.
19. Taglialatela, M. et al. 1992. Novel Voltage Clamp to Record Small, Fast Currents from Ion Channels Expressed in Xenopus Oocytes. Biophysical Journal. 61: 78-82.

Acknowledgements:

I thank my advisor Miguel Holmgren and all members of the Holmgren lab for assistance with oocyte harvesting, electrophysiology, and data analysis. Thank you to Deepa Srikumar for molecular biology and Carlos Gonzalez, Van Nguyen, and Angelica Lopez for assistance with electrophysiology. Thank you to Victoria Connaughton and Bill Parsons for help with data analysis and writing. This work was supported by the Intramural Research Program of the NIH, NINDS.